

# A further study of the (CR–LR) difference technique for retrospective radon exposure assessment

D. Nikezic<sup>a</sup>, C.W.Y. Yip<sup>a</sup>, S.Y.Y. Leung<sup>a</sup>, J.K.C. Leung<sup>b</sup>, K.N. Yu<sup>a,\*</sup>

<sup>a</sup>Department of Physics and Materials Science, City University of Hong Kong, Tat Chee Avenue, Kowloon Tong, Kowloon, Hong Kong

<sup>b</sup>Department of Physics, The University of Hong Kong, Pokfulam Road, Hong Kong

Received 29 July 2006; received in revised form 19 August 2006; accepted 21 August 2006

Available online 18 September 2006

## Abstract

The (CR–LR) difference technique, based on the CR-39 and LR 115 detectors, for the determination of implanted  $^{210}\text{Po}$  in glass after deposition of short-lived radon progeny, was analyzed in details in this paper. The sensitivities of both detectors were calculated using the Monte Carlo method with  $V$  functions particularly derived in our previous works for the detectors used in the present experiments. The dependency of the sensitivity ratio on the removed layer of both detectors was determined and verified experimentally. The simulated sensitivity ratios correlate well with the experimental ones. A major finding of the present work is that the sensitivity ratio between the CR-39 and LR 115 detectors depends only weakly on the ratio between the  $^{238}\text{U}$  and  $^{232}\text{Th}$  concentrations in the glass samples. This is crucial for the application of the (CR–LR) difference technique for retrospective radon exposure assessments, since measurements of the  $^{238}\text{U}$  and  $^{232}\text{Th}$  concentrations in the relatively small real-life glass samples will make the retrospective radon exposure assessments impractical.

© 2006 Elsevier B.V. All rights reserved.

PACS: 29.40; 23.60

Keywords: Radon; Radon progeny;  $^{210}\text{Po}$ ; Implantation; Retrospective dosimetry

## 1. Introduction

Methods for long-term passive radon measurements based on nuclear track detectors have been very well established and widely used. A survey of existing techniques has been given in Refs. [1,2]. Although these are classified as long-term measurement methods, the duration of measurements usually range between a few months to one year and are still too short compared to the average lifespan of a person. For risk estimation for a person, the total cumulative exposure is needed [3,4], so measurements performed for a few months might not be representative. As a possible solution to this problem, retrospective dosimetry based on measurements of  $^{210}\text{Po}$  activity in objects was proposed [5–7]. Distribution of implanted nuclei was studied in Ref. [8]. Exposures to  $^{222}\text{Rn}$  and its

progeny from the  $^{210}\text{Po}$  activity implanted in an object such as a glass object were investigated recently in Ref. [9].

To determine the activity of  $^{210}\text{Po}$  implanted in the surface of a glass object, the “(CR–LR) difference technique” was proposed [10]. The same method was also used in Ref. [11]. In this method, two detectors, namely, LR 115 and CR-39 were fixed side by side on the examined glass object. Since the CR-39 detector does not have an upper energy threshold, it can detect alpha particles emitted from the surface layer (originated from implanted  $^{210}\text{Po}$ ) as well as from the volume of an object. On the contrary, the LR 115 detector has an upper energy threshold that is well below 5.3 MeV which is the energy of alpha particles emitted by  $^{210}\text{Po}$  (except for removed layers larger than  $8\mu\text{m}$ , see discussions below) and it detects only alpha particles emitted from the volume. Therefore, the difference between the track densities on these two detectors (after correction for different sensitivities) can be used for measurements of  $^{210}\text{Po}$  implanted in

\*Corresponding author. Tel.: +852 27887812; fax: +852 27887830.

E-mail address: [peter.yu@cityu.edu.hk](mailto:peter.yu@cityu.edu.hk) (K.N. Yu).

the surface. The activity of  $^{210}\text{Po}$  ( $\text{Bq m}^{-2}$ ) is given in Refs. [10,11] as

$$A_{^{210}\text{Po}} = \frac{\text{CR} - B \times \text{LR}}{T \times K} \quad (1)$$

where CR is the net number of tracks per  $\text{cm}^2$  on the CR-39 detector, LR the net number of tracks per  $\text{cm}^2$  on the LR 115 detector,  $B$  the ratio of track densities recorded on a CR-39 detector to that on an LR 115 detector attached to a piece of unexposed glass,  $K$  the sensitivity factor for the CR-39 detector to surface  $^{210}\text{Po}$  activity (in the unit  $\text{tracks cm}^{-2}$  per  $\text{Bq h m}^{-2}$ ) and  $T$  the period of time (h) for which the CR-39 and LR 115 detectors are mounted on the glass surface.

This (CR–LR) difference technique was a pioneering and innovative method in the assessment of retrospective radon exposure. As described in Ref. [10], the technique “gave the correct value with a standard deviation of less than  $1 \text{ Bq m}^{-2}$ , which can be compared with results from a single measurement with one CR-39 detector”. Ref. [11] also described that the technique “has proven to be quite accurate and successful”. It is noticed that the parameters  $B$  and  $K$  depend on the employed etching conditions and readout procedures used in detector processing. The factor  $B$  was determined as 1.97 and  $K$  as  $0.081 \text{ tracks cm}^{-2} \text{ h per Bq m}^{-2}$  in Ref. [11]. However, the etching conditions and readout procedures were not given [10], so it is not straightforward to apply this technique.

In this paper, we would further study the (CR–LR) difference technique for retrospective radon exposure assessment, and would determine the parameters  $B$  and  $K$  for various removed layers from chemical etching for both the CR-39 and LR 115 detectors.

## 2. Methodology

### 2.1. Computer simulations

To calculate the parameter  $B$ , one needs the response of both the CR-39 and LR 115 detectors to different alpha-particle emitters in the volume of the glass object. On the other hand, to calculate the parameter  $K$ , one needs the response of the CR-39 detectors to  $^{210}\text{Po}$  on the surface of the glass object.

Let  $\rho_{\text{Ci}}$  and  $\rho_{\text{Li}}$  be the sensitivities (in the unit  $[\text{tracks m}^{-2}]/[\text{Bq m}^{-3} \text{ s}]$  or simply [m]) of the CR-39 and the LR 115 detectors, respectively, to the  $i$ th alpha emitter in the volume of the glass object, for particular removed layers of the CR-39 and the LR 115 detectors. The number of tracks on the CR-39 and the LR 115 detectors are denoted by  $N_{\text{C}}$  and  $N_{\text{L}}$ , respectively, and are given by

$$N_{\text{C}} = \sum_i \rho_{\text{Ci}} \times A_i t \quad \text{and} \quad N_{\text{L}} = \sum_i \rho_{\text{Li}} \times A_i t \quad (2)$$

and therefore

$$B = \frac{N_{\text{C}}}{N_{\text{L}}} = \frac{\sum_i \rho_{\text{Ci}} \times A_i t}{\sum_i \rho_{\text{Li}} \times A_i t} \quad (3)$$

where  $A_i$  is the specific activity (in the unit  $[\text{Bq m}^{-3}]$ ) of the  $i$ th alpha emitter in the volume of the glass object, and  $t$  the exposure time. Apparently,  $B$  is dependent on the specific activities of the different alpha emitters. Members of the two natural radioactive chains of  $^{232}\text{Th}$  and  $^{238}\text{U}$  can be found in freshly manufactured glass samples. A total of 12 species of alpha particles (with different energies) are emitted in the  $^{238}\text{U}$  series and 11 in the  $^{232}\text{Th}$  series (some branches with minor branching ratios are neglected). These alpha-particle energies and the corresponding branching ratios are given in Table 1. The total sensitivity is obtained under the assumption that all members of  $^{238}\text{U}$  and  $^{232}\text{Th}$  are in equilibrium. The sensitivities of individual radionuclides were weighted according to the branching ratios and then summed up.

Monte Carlo programs previously developed for calculation of detector responses to radon and its progeny in air and described in Refs. [12,13] were modified and applied to the case for  $^{210}\text{Po}$  in glass. Details of the program are not repeated here. In the simulations, at least  $10^5$  events were used so the statistical uncertainty is very small. The stopping powers and ranges of alpha particles in glass were calculated using the SRIM-2003 code [14]. Calculations were carried out for “Glass Soda Lime” with the density of  $2.33 \times 10^3 \text{ kg m}^{-3}$  (listed in “Common implantation materials” in the SRIM-2003 directory). The stopping powers and ranges of alpha particles in LR 115 and CR-39 detectors were also calculated by the SRIM-2003 code.

To perform calculations for the detector sensitivities, the corresponding  $V$  functions are needed. The  $V$  function is defined as the ratio between track etch rate  $V_t$  and the bulk etch rate  $V_b$ , i.e.,  $V = V_t/V_b$ . It is usually expressed as a function of the residual range  $R'$  of the alpha particles in the detector material. We used the  $V(R')$  functions specifically determined for the CR-39 and LR 115 detectors

Table 1  
Energies and branching ratios of alpha particles emitted from the  $^{238}\text{U}$  and  $^{232}\text{Th}$  and radioactive decay series

$^{238}\text{U}$		$^{232}\text{Th}$	
$E_x$ (MeV)	Branching ratio	$E_x$ (MeV)	Branching ratio
4.151	0.209	3.947	0.217
4.198	0.79	4.012	0.782
4.601	0.0555	5.423	0.722
4.6205	0.234	5.34	0.272
4.687	0.763	5.4486	0.0606
4.7224	0.2824	5.6854	0.9492
4.7746	0.7138	6.05	0.248
4.784	0.9445	6.09	0.0965
5.3	1	6.288	1
5.4897	1	6.788	1
6.002	1	8.78	1
7.686	1		

being used in the present experiments. The  $V$  function for the LR 115 detector has a form given in Ref. [15] as

$$V = 1 + \left( A_1 e^{-A_2 R'} + A_3 e^{-A_4 R'} \right) \left( 1 - e^{-R'} \right)$$

where the parameters were found in Ref. [16] as  $A_1 = 14.50$ ,  $A_2 = 0.5$ ;  $A_3 = 3.9$  and  $A_4 = 0.066$  for LR 115 detector, and  $R'$  is the residual range of alpha particles in the LR 115 detector. On the other hand, the  $V$  function for CR-39 adopted functional form proposed in Ref. [17]:

$$V = 1 + e^{-C_1 R' + C_4} - e^{-C_2 R' + C_3} + e^{C_3} - e^{C_4}$$

with the constants  $C_1 = 0.06082$ ,  $C_2 = C_4 = 1.119$  and  $C_3 = 0.8055$  obtained from our previous work [18].

## 2.2. Experimental methodology

The LR 115 detectors used in the present study were purchased from DOSIRAD, France (LR 115 film, Type 2, nonstrippable). The detectors consist of an active layer of red cellulose nitrate on a 100  $\mu\text{m}$  clear polyester base substrate. After the desired exposure, the detectors were etched in a 2.5 N aqueous solution of NaOH maintained at a 60  $^\circ\text{C}$  by a water bath, which is a frequently used etching condition for the LR 115 detector. The temperature was kept constant with an accuracy of  $\pm 1$   $^\circ\text{C}$ . The detectors were etched using a magnetic stirrer (Model no: SP72220-26, Barnstead/Thermolyne, IA, USA).

The bulk etch rate of the LR 115 detector could not be controlled by the etching temperature and the etchant concentration only, but was also affected by the amount of stirring [19]. Therefore, actual monitoring of the active-layer thickness is necessary when using the LR 115 detector. In the present paper, the thickness of the active layer of the LR 115 detector was obtained from the infrared transmittance [20]. Other fast and convenient methods to obtain the thickness of the active layer of the LR 115 detector include the use of Energy-Dispersive X-ray Fluorescence (EDXRF) [21] or determination of the optical density using a color commercial document scanner [22]. After etching, the detectors were removed from the etchant and immediately rinsed by distilled water. After drying, the detectors were scanned using a Perkin Elmer Fourier Transform Infrared (FTIR) spectroscopy system (Model 16 PC FT-IR) for 10 cycles. The wave number range employed was between 1700 and 1100  $\text{cm}^{-1}$ , with a resolution of 4  $\text{cm}^{-1}$ . The scanned diameter was 9 mm so the scanned area was 0.64  $\text{cm}^2$ . The infrared transmittance at the wave number at 1598  $\text{cm}^{-1}$  (corresponding to the O–NO<sub>2</sub> bond) was measured and the relationship from Ref. [20] was used to give the corresponding thickness of the active layer for LR 115 detector. Four LR 115 detectors were used in the experiments. The removed layers were determined to be  $(5.06 \pm 0.09)$ ,  $(5.28 \pm 0.03)$ ,  $(5.86 \pm 0.24)$  and  $(5.90 \pm 0.06)$   $\mu\text{m}$ .

The CR-39 detectors used in the present study were purchased from Page Mouldings (Pershore) Limited

(Worcestershire, England). The detectors were etched in 6.25 N NaOH maintained at 70  $^\circ\text{C}$  by a water bath, which is a frequently used etching condition for CR-39 detectors. The temperature was kept constant with an accuracy of  $\pm 1$   $^\circ\text{C}$ . The detectors were etched with no stirring, and the bulk etch rate was found to be relatively constant at 1.2  $\mu\text{m h}^{-1}$  [23]. One CR-39 detector was used in the experiments with a removed layer of 7.2  $\mu\text{m}$ .

## 3. Results

### 3.1. Ratio $B$ in Eq. (1)

#### 3.1.1. Sensitivity of the LR 115 detector to alpha emitters in natural decay series in glass volume

The sensitivities of the LR 115 detector to alpha particles with the energies listed in Table 1 emitted in the glass volume are given in Fig. 1, with the removed layer as a parameter. One can see that the sensitivity of the LR 115 detector is independent of the alpha-particle energy for smaller removed layers (4, 5 and 6  $\mu\text{m}$ ). This is also true for larger removed layers (7 and 8  $\mu\text{m}$ ) except for alpha energies below some critical values which depend on the removed layer. Equality of partial sensitivities was observed for alpha particles emitted in air from <sup>222</sup>Rn and its short-lived progeny, which was discussed in details in Ref. [24]. The equality of partial sensitivities to radon progeny in air is a consequence of the presence of upper and lower energy thresholds for the LR 115 detector for registration of alpha particles [25]. This equality of partial sensitivities is impaired for lower alpha-particle energies and for larger removed layers.

The total sensitivities of the LR 115 detector to alpha emitters in both natural decay series in glass as a function

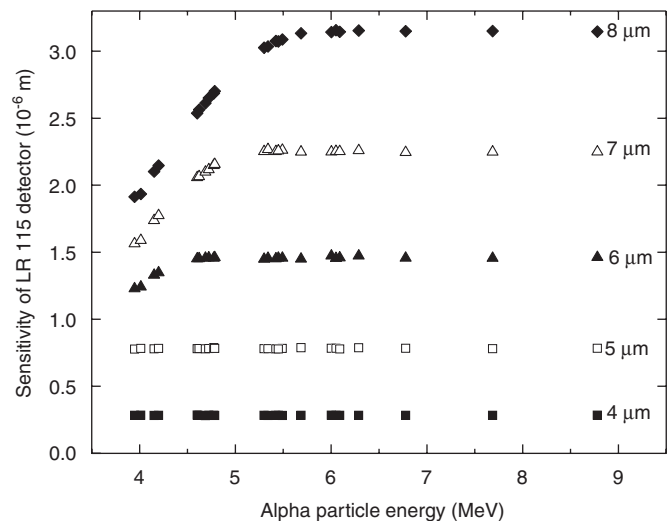


Fig. 1. Partial sensitivities (in m) of the LR 115 detector to alpha particles emitted in the glass volume from the natural radioactive series, with removed layer (shown on the right of the curves) as a parameter, as determined using Monte Carlo simulations. The initial active layer thickness of the detector is assumed to be 12  $\mu\text{m}$ .

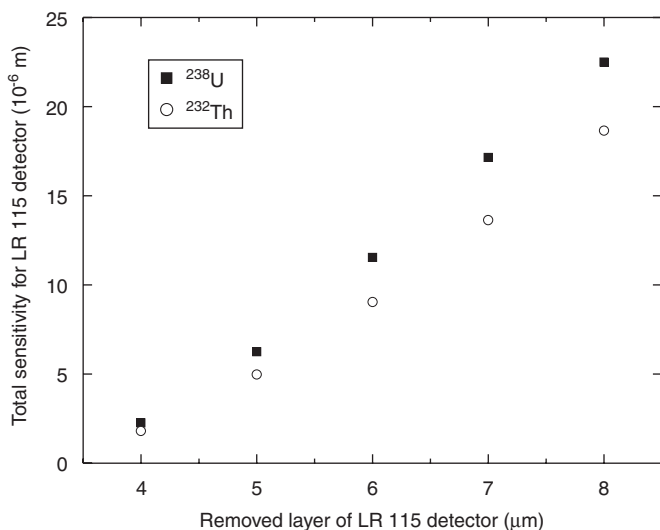


Fig. 2. Total sensitivity (in m) of the LR 115 detector to alpha particles emitted in the glass volume from the natural radioactive series of  $^{238}\text{U}$  and  $^{232}\text{Th}$ , with removed layer as a parameter, as determined using Monte Carlo simulations. The initial active layer thickness of the detector is assumed to be  $12\ \mu\text{m}$ .

of the removed layer are given in Fig. 2. In the calculations, only fully perforated tracks were taken into consideration. It is interesting to note in Fig. 2 that the sensitivities to the  $^{238}\text{U}$  series are larger than those to the  $^{232}\text{Th}$  series, despite the same partial sensitivities, because the branching ratios and the number of alpha particle species are different for the series.

One can notice the significant dependence of the detector sensitivity on the removed layer of the LR 115 detector. Except for the data for the removed layer of  $4\ \mu\text{m}$ , the dependence is almost linear. This is also related to the presence of the upper and lower energy thresholds for registration of alpha particles for this detector. With prolonged etching, the energy window widens so the detector sensitivity increases significantly. The variations of the upper and lower energy thresholds with the removed layer are shown in Fig. 3. It is remarked that the energy thresholds are dependent on the  $V$  function used in the calculations.

### 3.1.2. CR-39 detector sensitivity to alpha emitters in glass volume

In contrast to the LR 115 detector, the upper energy threshold of the CR-39 detector is greater than  $20\ \text{MeV}$ , which is much larger than the largest alpha-particle energy ( $7.68\ \text{MeV}$ ) from radon progeny and that ( $8.78\ \text{MeV}$ ) from thoron progeny. Therefore, for the purpose of recording alpha particles from the  $^{238}\text{U}$  and  $^{232}\text{Th}$  series, including radon, thoron and their progeny, CR-39 detectors effectively do not have an upper energy threshold.

Unlike the case for the LR 115 detector for which we use complete perforation of the active layer as the visibility criterion, it is necessary to establish a visibility criterion for the CR-39 detector, i.e., the size and depth of a track when it becomes visible under the optical microscope. In the

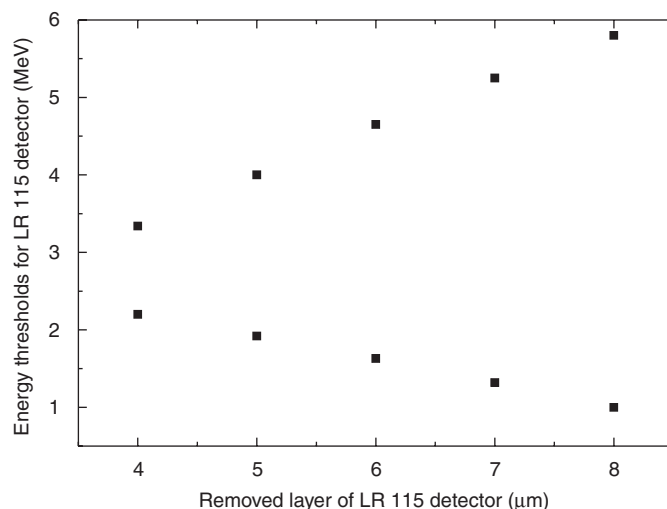


Fig. 3. Variations with the removed layer of the upper energy threshold (upper set of data) and lower energy threshold (lower set of data) for the LR 115 detector.

present calculations, we adopted the criteria that the tracks whose major or minor axes are smaller than  $1\ \mu\text{m}$  or whose depths are smaller than  $1\ \mu\text{m}$  are invisible under the microscope. With prolonged etching, the tracks become larger so one can expect a larger number of tracks to satisfy the criteria. However, the track depth does not increase beyond a certain value which is related to the alpha-particle range in the detector material. This has been shown experimentally in previous works [26]. In this situation, even though the major and minor axes of the track opening increase with prolonged etching, the depth remains the same, and the number of “visible” tracks does not increase. In other words, the detector sensitivity should come to saturation. If a very long etching period is applied, the alpha-particle tracks will go into the rounded phase; their images will then lose the optical contrast and the tracks might become invisible again.

The relationship between the CR-39 sensitivity and the alpha-particle energy is shown in Fig. 4, which is slightly nonlinear (in contrast to the relationship in the case of the LR 115 detector). On the other hand, the dependence on the removed layer is weak, which is more pronounced in the higher alpha-particle energy region.

The total sensitivity to alpha emitters in the glass volume is given in Fig. 5 as a function of the removed layer thickness. Saturation of the CR-39 detector sensitivity can be noticed. The sensitivities to the two decay chains are not the same although they are close to each other. Similarly to the previous case for the LR 115 detector, the  $^{238}\text{U}$  series will produce more alpha-particle tracks in the CR-39 detector than the  $^{232}\text{Th}$  series. These features are the consequences of the complicated interplay between the different numbers of alpha particle species emitted in the two series, the different average energies in the two series ( $5.36\ \text{MeV}$  in the  $^{238}\text{U}$  series and  $6.15\ \text{MeV}$  in the  $^{232}\text{Th}$  series), and the increase in the sensitivity with alpha-particle energy and

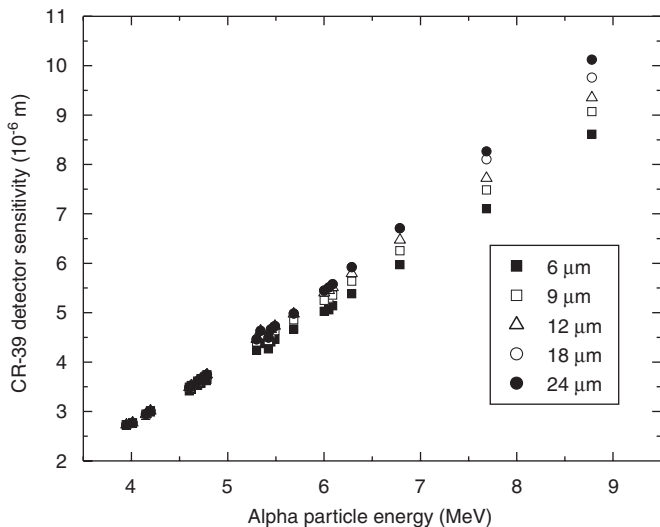


Fig. 4. Partial sensitivities (in m) of the CR-39 detector to alpha particles emitted in the glass volume from the natural radioactive series, with removed layer as a parameter, as determined using Monte Carlo simulations.

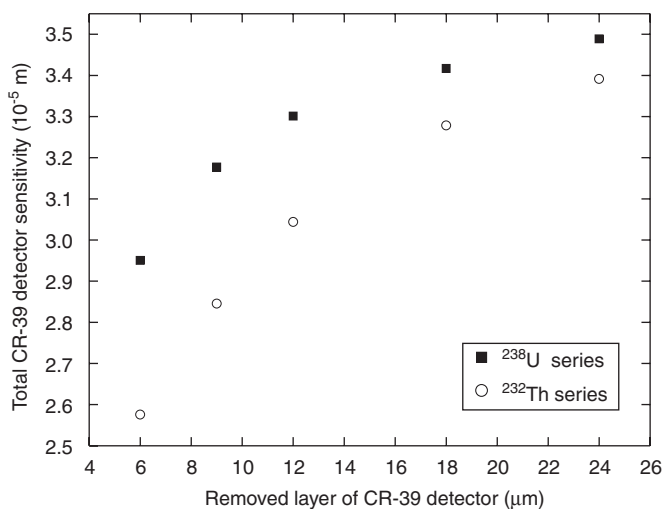


Fig. 5. Total sensitivity (in m) of the CR-39 detector to alpha particles emitted in the glass volume from the natural radioactive series of  $^{238}\text{U}$  and  $^{232}\text{Th}$ , with removed layer as a parameter, as determined using Monte Carlo simulations.

the removed layer of the detector. In the lower alpha-particle energy region and for smaller removed layers of the detector, the sensitivities are close to each other (see Fig. 4), and the larger number of alpha particles emitted in the  $^{238}\text{U}$  series leads to a larger detector sensitivity. In the higher alpha-particle energy region, the higher average alpha-particle energy in the  $^{232}\text{Th}$  series (which means larger detection efficiencies) partially compensates for the lower number of alpha particles emitted in this series, and two curves tend to converge to each other.

### 3.1.3. Ratio *B*

The ratio *B* between the track densities recorded on a CR-39 detector and that on an LR 115 detector attached to

a piece of unexposed glass, which are given in Figs. 2 and 5, respectively, were calculated for different combinations of removed layer thickness of the detectors, and the results are presented in Table 2. Here, three different ratios between the activities of the radionuclides in the  $^{238}\text{U}$  series and the  $^{232}\text{Th}$  series, namely, 1:1, 1:9 and 9:1. It is noted that *B* depends only weakly on these ratios, which is crucial for the practicability of the (CR–LR) difference technique for retrospective radon exposure assessments. The requirement to measure the  $^{238}\text{U}$  and  $^{232}\text{Th}$  concentrations in the relatively small real-life glass samples will make the retrospective radon exposure assessment technique impractical.

For a fixed removed layer of the CR-39 detector (columns in Table 2), the ratio of sensitivities decreases rapidly with increases in the removed layer of the LR 115 detector. For a fixed removed layer of the LR 115 detector (rows in Table 2), the ratio increases with the removed layer of the CR-39 detector, but the increase is not very significant. Some ratios for the removed layer of 4 μm for the LR 115 detector are too large, but the results for the removed layer of 4 μm are still included in Table 2; the large values are due to the very small sensitivities of the LR 115 detectors for small removed layers where the majority of tracks are not fully etched.

### 3.1.4. Experimental verification

In this part, experimental verification of the ratios between the sensitivities will be carried out. LR 115 and CR-39 detectors were attached to fresh glass objects for about seven months. The size of the detectors used were all  $3 \times 3 \text{ cm}^2$ .

After the chemical etching of both detectors as described in Section 2.2, the track densities were determined by manually counting the number of tracks on the detectors under the optical microscope, and by subtracting the background track densities determined from unirradiated detectors. The same criteria were used in actual counting as in theoretical calculations. The ratios of track densities were then calculated. The results are presented in Fig. 6. The error bars for the experimental values represent one standard error. In the simulations, at least  $10^5$  events were used so the statistical uncertainties are very small and are thus not shown. The calculations have assumed that both the decay series of  $^{238}\text{U}$  and  $^{232}\text{Th}$  have the same activity. The calculated CR-39 sensitivity for a removed layer of 7.2 μm is  $2.86 \times 10^{-5} \text{ m}$  while the calculated LR 115 sensitivities for the removed layers of 5.06, 5.28, 5.86 and 5.90 μm were  $0.589 \times 10^{-5}$ ,  $0.692 \times 10^{-5}$ ,  $0.963 \times 10^{-5}$  and  $0.982 \times 10^{-5} \text{ m}$ , respectively. Therefore, the calculated ratios are 4.86, 4.13, 2.97 and 2.91, respectively. The experimentally obtained ratios are 4.40, 4.50, 2.50 and 3.76. The correlation coefficient between the experimental and calculated results was determined as 0.76, which demonstrates a strong correlation between the experimental and calculated values.

Table 2

The ratios  $B$  between the track densities recorded on a CR-39 detector and that on an LR 115 detector attached to a piece of unexposed glass, calculated for different combinations of removed layer thickness of the detectors

Removed active layer in LR 115 ( $\mu\text{m}$ )	Removed layer in CR-39 detector ( $\mu\text{m}$ )				
	6	9	12	18	24
4	13.6 (13.2;14.1)	14.8 (14.2;15.6)	15.6 (14.8;16.6)	16.5 (15.4;17.8)	16.9 (15.7;18.4)
5	4.9 (4.7;5.1)	5.4 (5.1;5.6)	5.6 (5.3;6.0)	5.9 (5.5;6.4)	6.3 (5.6;6.7)
6	2.7 (2.6;2.8)	2.9 (2.7;3.1)	3.1 (2.9;3.3)	3.2 (3.0;3.5)	3.3 (3.1;3.7)
7	1.8 (1.7;1.9)	1.9 (1.8;2.1)	2.1 (1.9;2.2)	2.2 (2.0;2.3)	2.2 (2.1;2.4)
8	1.3 (1.3;1.4)	1.4 (1.4;1.5)	1.5 (1.5;1.6)	1.6 (1.5;1.7)	1.6 (1.6;1.8)

The ratios outside the brackets are obtained assuming that the radionuclides in both the  $^{238}\text{U}$  and  $^{232}\text{Th}$  series have the same activities, where arithmetic average sensitivities have been used. The ratios inside the brackets are obtained assuming different ratios between the activities of the radionuclides in the  $^{238}\text{U}$  series and the  $^{232}\text{Th}$  series (1:9 for the first numbers, and 9:1 for the second numbers).

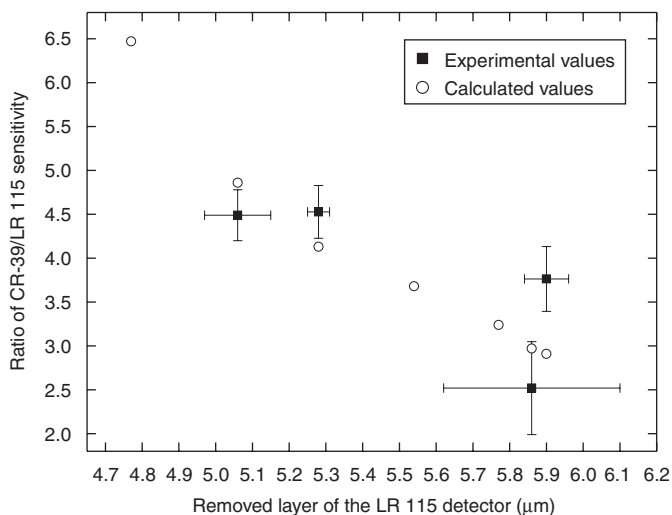


Fig. 6. Ratios between the sensitivities (for CR-39 and LR115 detectors): experimental values (squares) and calculated values (open circles). The error bars represent one standard errors.

### 3.2. Sensitivity $K$ in Eq. (1)

To determine the constant  $K$  in Eq. (1), the same Monte Carlo programs were used with modifications in the sampling of initial points of alpha particles. Here, the alpha particles are emitted just on the surface of the glass. Since the detector is in contact with the glass, half of the emitted alpha particles will enter the detector. As a first approximation, one can take that the detector efficiency as about 50% in this case. However, due to the existence of critical angles for detection, not all alpha particles would be registered. Table 3 shows the results for the factor  $K$  as a function of the removed layer of the CR-39 detector.

It was proposed in Ref. [10] that  $K = 0.081 \text{ track cm}^{-2}$  per  $\text{Bq h m}^{-2}$ , which was subsequently adopted by Ref. [11]. This result was obtained for “standard” procedures, but these conditions and procedures were not described in Ref. [10]. The calculations for our etching conditions (7  $\mu\text{m}$  of removed layer) and readout procedures give  $K = 0.17 \text{ (track m}^{-2}\text{)/(Bq s m}^{-2}\text{)}$ , or  $0.059 \text{ (track cm}^{-2}\text{)/(Bq h/m}^2\text{)}$ ,

Table 3

The factor  $K$  as a function of the removed layer of the CR-39 detector

Removed layer of CR-39 ( $\mu\text{m}$ )	$K \text{ (track m}^{-2}\text{)/(Bq s m}^{-2}\text{)}$	$K \text{ (track cm}^{-2}\text{)/(Bq h m}^{-2}\text{)}$
6	0.147	0.059
9	0.193	0.069
12	0.281	0.101
18	0.282	0.102

which is close to the value of  $0.081 \text{ (track cm}^{-2}\text{)/(Bq h m}^{-2}\text{)}$  given in Ref. [10]. The statistical uncertainty for our calculated  $K$  values is 1% or smaller.

## 4. Conclusions and discussion

The (CR–LR) difference technique, based on the CR-39 and LR 115 detectors, for the determination of implanted  $^{210}\text{Po}$  in glass after deposition of short-lived radon progeny, was analyzed in this paper. The sensitivities of both detectors were calculated using the Monte Carlo method with  $V$  functions particularly derived in our previous works for the detectors used in the present experiments. The dependence of the sensitivity ratio on the removed layer of both detectors was determined and verified experimentally. The simulated sensitivity ratios correlate well with the experimental ones.

A major finding of the present work is that the sensitivity ratio between the CR-39 and LR 115 detectors depends only weakly on the ratio between the  $^{238}\text{U}$  and  $^{232}\text{Th}$  concentrations in the glass samples. This is crucial for the application of the (CR–LR) difference technique for retrospective radon exposure assessments, since measurements of the  $^{238}\text{U}$  and  $^{232}\text{Th}$  concentrations in the relatively small real-life glass samples will make the retrospective radon exposure assessments impractical.

The sensitivity of the LR 115 detector significantly depends on the removed layer; e.g., it is increased by a factor of two if the etched layer was increased from 5 to 6  $\mu\text{m}$ . This highlights the necessity to accurately monitor

the removed layer of the LR 115 detector, particularly because it is established that the removed layer of the LR 115 detector depends on the amount of stirring during the chemical etching and cannot be surrogated by the etching conditions alone. However, this caution is not only restricted to the (CR–LR) difference technique described here, but is instead applicable to all applications of the LR 115 detector such as those in routine radon gas measurements. On the other hand, the sensitivity of the CR-39 detector is less dependent on the removed layer, and even achieves saturation for removed layers larger than 20  $\mu\text{m}$ . Therefore, controlling of its removed layer is less critical.

### Acknowledgment

This research was supported by a grant from the Research Grants Council of the Hong Kong Special Administrative Region, China [Project No. CityU 103204].

### References

- [1] V.A. Nikolaev, R. Ilic, *Radiat. Meas.* 30 (1999) 1.
- [2] D. Nikezic, K.N. Yu, *Mater. Sci. Eng. R* 46 (2004) 51.
- [3] F. Bochicchio, F. Forastiere, S. Farchi, D. Marocco, M. Quarto, F. Sera, *Radiat. Meas.* 36 (2003) 205.
- [4] D. Nikezic, K.N. Yu, *Radiat. Prot. Dosim.* 113 (2005) 233.
- [5] C. Samuelsson, *Nature* 334 (1988) 338.
- [6] R.S. Lively, E.P. Ney, *Health Phys.* 52 (1987) 411.
- [7] J.A. Mahaffey, M.A. Parkhurst, A.C. James, F.T. Cross, M.C.R. Alavanja, J.D. Boice, S. Ezrine, P. Henderson, R.C. Brownson, *Health Phys.* 64 (1993) 381.
- [8] B. Roos, H.J. Whitlow, *Health Phys.* 84 (2003) 72.
- [9] D. Nikezic, K.N. Yu, *Radiat. Meas.* 41 (2006) 101.
- [10] R. Falk, H. Mellander, L. Nyblom, I. Östergren, *Environ. Int.* 22 (Suppl. 1) (1996) S857.
- [11] J.P. McLaughlin, *Radiat. Prot. Dosim.* 78 (1998) 1.
- [12] D. Nikezic, K.N. Yu, *Radiat. Meas.* 37 (2003) 39.
- [13] D. Nikezic, K.N. Yu, *Comput. Phys. Commun.* 174 (2006) 160.
- [14] J.F. Ziegler, SRIM-2003, 2003. <<http://www.srim.org/>>.
- [15] S.A. Durrani, P.F. Green, *Nucl. Tracks* 8 (1984) 21.
- [16] S.Y.Y. Leung, D. Nikezic, J.K.C. Leung, K.N. Yu, *Appl. Radiat. Isot.*, 2006, in press.
- [17] C. Brun, M. Fromm, M. Jouffroy, P. Meyer, J.E. Groetz, F. Abel, A. Chambaudet, B. Dorschel, D. Hermsdorf, R. Bretschneider, K. Kadner, H. Kuhne, *Radiat. Meas.* 31 (1999) 89.
- [18] K.N. Yu, F.M.F. Ng, D. Nikezic, *Radiat. Meas.* 40 (2005) 380.
- [19] C.W.Y. Yip, J.P.Y. Ho, V.S.Y. Koo, D. Nikezic, K.N. Yu, *Radiat. Meas.* 37 (2003) 197.
- [20] F.M.F. Ng, C.W.Y. Yip, J.P.Y. Ho, D. Nikezic, K.N. Yu, *Radiat. Meas.* 38 (2004) 1.
- [21] C.W.Y. Yip, J.P.Y. Ho, D. Nikezic, K.N. Yu, *Radiat. Meas.* 36 (2003) 161.
- [22] K.N. Yu, F.M.F. Ng, *Nucl. Instr. and Meth. B* 226 (2004) 365.
- [23] J.P.Y. Ho, C.W.Y. Yip, D. Nikezic, K.N. Yu, *Radiat. Meas.* 36 (2003) 141.
- [24] K.N. Yu, D. Nikezic, F.M.F. Ng, J.K.C. Leung, *Radiat. Meas.* 40 (2005) 560.
- [25] D. Nikezic, F.M.F. Ng, K.N. Yu, *Appl. Radiat. Isot.* 61 (2004) 1431.
- [26] B. Dorschel, D. Füll, H. Hartmann, D. Hermsdorf, K. Kadner, C. Radlach, *Radiat. Prot. Dosim.* 69 (1997) 267.